Mathematical Model for the Study of Mitochondrial Retrograde Signaling Dynamics

Shao-Ting Chiu[1], **Wen-Wei Tseng**[1], **An-Chi Wei**[1]

Affiliation: [1]Graduate Institute of Biomedical Electronics and Bioinformatics, National Taiwan University, Taipei, Taiwan
Correspondence: acwei86@ntu.edu.tw (A. W.)

Summary

Mitochondria are semi-autonomous eukaryotic organelles, that participate in energy production and metabolism, making mitochondrial quality control crucial. As most mitochondrial proteins are encoded by nuclear genes, quality control depends on proper mitochondria-nucleus communication, designated mitochondrial retrograde signaling. Early studies focused on retrograde signaling participants and specific gene knockouts. However, mitochondrial signal modulation remains elusive. Using yeast, we simulated signal propagation following mitochondrial damage and proposed a mathematical model based on enzyme kinetics and ordinary differential equations. Mitochondrial retrograde signaling decisions were described by a Boolean model. Dynamics were analyzed through an ordinary differential equation-based model and extended to evaluate the model response to noisy damage signals. Simulation revealed localized protein concentration dynamics, including waveforms, frequency response, and robustness under noise. Retrograde signaling is bistable with three localized steady states, while increased damage compromises robustness. We elucidated mitochondrial retrograde signaling, providing a basis for drug design against yeast and fungi.

Keywords

Mitochondrial retrograde signaling (RTG), mathematical modeling, control systems

---

Introduction

Mitochondria serve as the cells' powerhouse, utilizing the established proton motive force to generate the high-energy molecule, ATP, thus facilitating various cellular processes (Osellame et al.

2012). The analogy of a simple electrical circuit model is a convenient way to describe the interactions between ion dynamics and energetics in the complex mitochondrial system (Friedman & Nunnari 2014). Mitochondria regulate various cellular mechanisms under normal physiological conditions, as well as disease, including ATP generation, regulation of signal transduction, immune responses, and cell apoptosis (Osellame et al. 2012). Therefore, mitochondria serve as an essential regulatory metabolic hub (Mottis et al. 2019).

However, their extensive role within the cell renders mitochondria prone to be damaged (Liu & Butow 2006, Ždralević et al. 2012). Mitochondrial quality control is therefore essential for cell viability, which relies on mitochondria-driven energy production (Osellame et al. 2012), lipid synthesis (Aon et al. 2014), and amino acid metabolism (King 2007). However, energy production via the electron transport chain results in an oxidative stress burden (Knorre et al. 2016). Unlike other membrane-bound organelles, which rely solely on protein products from the nuclear genome, mitochondria possess their own genome, encoding dedicated enzymes and repair systems; however, remain semi-autonomous organelles, as most mitochondria protein-encoding genes are translocated into the nucleus (Gabaldón & Huynen 2004). In fact, in budding yeast, only 35 of the 1000 mitochondrial genes are located in the mitochondrial genome, representing a minor fraction of the metabolic system (Malina et al. 2018). Therefore, mitochondria require various nuclear gene products to maintain functionality. The interaction between mitochondria and the nucleus is a bidirectional process (Da Cunha et al. 2015, Mottis et al. 2019). Once mitochondria are damaged, their status is reported to the nucleus via signaling factors or metabolic system interference, enabling the cell to coordinate mitochondrial biogenesis. Furthermore, mitochondrial quality control depends on mitochondrial feedback, referred to as mitochondrial retrograde (RTG) signaling (Butow & Avadhani 2004, Cagin & Enriquez 2015, Da Cunha et al. 2015, Liu & Butow 2006).

The most well-characterized mitochondrial RTG signaling cascade is that in budding yeast (Chelstowska et al. 1999, Da Cunha et al. 2015, Jazwinski & Kriete 2012, Liao & Butow 1993, Sekito et al. 2000), which becomes triggered when mitochondrial respiratory function is compromised (Epstein et al. 2001), causing a shift in carbohydrate and nitrogen metabolism (Liu & Butow 1999). *CIT2*, one of the regulated genes, encodes a peroxisomal isoform of citrate syntheses involved in the glyoxylate cycle, thereby bypassing the TCA cycle. Thus, the upregulation of *CIT2* allows for more efficient usage of carbon sources when mitochondria are damaged. This RTG pathway was first characterized by investigating various yeast gene deletion strains. For instance, in (Sekito et al. 2000), RTG genes were independently knocked out, and green fluorescent protein (GFP) was employed to localize RTG proteins, revealing details of the mitochondria-to-nucleus communication system (Figure 1). Further, the localization of RTG proteins was compared among deletion strains, as well as strains with dysfunctional mitochondria, such as ρ^0 cells, which lack a mitochondrial genome.

The RTG pathway is started with Rtg2p, a cytoplasmic sensor of mitochondrial damage. Rtg2p

is activated by the loss of mitochondrial membrane potential or the ATP/ADP ratio, and the activation results in the degradation of Bmhp/Mksp heterodimer that inhibits the Rtg3p activation (Ferreira et al. 2005, Liao & Butow 1993). The Rtg1p/3p are transcription factors that turning on the retrograde response by nucleus translocation with nucleus localization signal (NLS) (Jazwinski 2013).

Without Rtg2p sensing mitochondrial status, Rtg3p and Rtg1p localization occurs independently of mitochondrial damage due to constant inhibition of Mksp. Rtg3p and Rtg1p remain cytoplasmic in wild type and dysfunctional mitochondria (ρ^0 strain) (Sekito et al. 2000). In addition, Rtg1p regulates the translocation of Rtg3p. While Rtg1p participates in the activation of the retrograde response, it retains Rtg3p in the cytoplasm in the absence of mitochondrial damage. In contrast, Rtg3p accumulates in the nucleus regardless of mitochondrial status in Rtg1p knockout mutants, while the opposite is not true. Initiation of retrograde response signaling requires nuclear accumulation of both Rtg3p and Rtg1p, which are basic helix-loop-helix (bHLH) transcription factors that regulate retrograde response genes like the AND logic gate (Hashim et al. 2014, Rothermel et al. 1997, Sekito et al. 2000). Therefore, Rtg1p acts as a positive regulator of retrograde response genes, as well as a negative regulator that retains Rtg3p in the cytoplasm in the absence of mitochondrial damage.

Cells usually harbor a number of mitochondria that share the same retrograde signaling pathway, resulting in a multiplexing issue first described in telecommunications (Cover & Thomas 2005). Sharing signaling channels may lead to unwanted crosstalk. Further, biochemical pathway noise restricts the cells' ability to receive information from their organelles. In eukaryotic cells, such as budding yeast, mitochondria interact with the nucleus via the same biochemical channels, while the consequent multiplexing issue represents a barrier to assessing the health state of each mitochondrion. How biological systems manage multiplex communication networks during the mitochondrial RTG response remains unclear.

The RTG response facilitates the adaptation of eukaryotic organisms to unfavorable factors (Fatima et al. 2020, Trendeleva & Zvyagilskaya 2018). In yeast, the key role of RTG signaling is the regulation of mitochondrial function and metabolic reprogramming, including the maintenance of intracellular glutamate supplies (Liu et al. 2002, Trendeleva & Zvyagilskaya 2018). Recently, several studies have reported the association between the retrograde response and drug resistance in yeast (Hans et al. 2019, Moye-Rowley 2005, Trendeleva & Zvyagilskaya 2018). For example, Rtg3p was reported as essential for antifungal drug tolerance associated with the formation of the fungal plasma membrane, which contains ergosterol (Yan et al. 2014). Also, the Δ*rtg3* mutant of pathogenic yeast, *Candida albicans*, exhibits compromised biofilm formation and epithelial cell adherence, resulting in reduced infectivity of *C. elegans* (Hans et al. 2019). Meanwhile, in *S. cerevisiae*, pleiotropic drug resistance (PDR) is activated by RTG signaling, inducing the transcription of PDR genes (Trendeleva & Zvyagilskaya 2018). RTG signaling is also associated with aging, highlighting yeast as a model organism for the study of mitochondrial quality control and its influences

on lifespan (Jazwinski 2013).

To investigate the communication properties of mitochondrial retrograde signaling, we developed a differential equation-based model to simulate the process. The mitochondrial status, and deleted genes, are defined as input, whereas translocation of Rtg1p/Rtg3p is the defined output. These interactions were previously observed via microscopy by (Sekito et al. 2000, 2002), and subsequently summarized in a Boolean table. The parameters were fitted with the Boolean relationship using Monte Carlo simulation. A parameter set was verified by solving the steady states under each observed genotype. Taken together, our mathematical model interprets the dynamics of mitochondrial retrograde signaling. Furthermore, the proposed mathematical model also has potential applications in research on antifungal drugs and aging.

Results

A differential equation-based model of mitochondrial retrograde signaling

As a channel of communication between mitochondria and the nucleus, RTG signaling is well regulated and fine-tuned for a proper response to mitochondrial damage signals. The dynamics and interactions of Rtg1p, Rtg2p, Rtg3p, Msk1p, and Bmhp can be described by ordinary differential equations (ODE) and chemical kinetics. The first part of RTG signaling is the activation layer, during which the mitochondrial damage signal activates Rtg2p. The signal is then transmitted to the modulation layer where Rtg1/3p translocate into the nucleus and initiate transcription (Figure 1). For simplicity, the chemical interactions among retrograde proteins and the translocation of Rtg1/3p are assumed to obey the law of mass action, and the total concentration of each protein is regarded as conserved. To connect retrograde proteins with mitochondrial damage, the activation of Rtg2p was modeled using the Hill equation with the sum of mitochondrial damage (s in Figure 1). Furthermore, proteins with activation states or locations are defined separately, leading to a total of 17 protein variables and 24 kinetic coefficients (Figure 1).

To identify the parameter set that would make the model compatible with previous research (Ghaemmaghami et al. 2003, Sekito et al. 2000, 2002), a Monte Carlo simulation method was used to perform the parameter exploration. First, to leverage the microscopic data from (Sekito et al. 2000) and (Sekito et al. 2002), the translocation of Rtg1/3p and mitochondrial states were summarized in a Boolean model with 17 genetic backgrounds, including the combination of RTG gene knockouts (See STAR*Methods). Second, the differential expressions of Bmhp and Rtg1/2/3p were determined based on the quantitative western blot analysis from (Ghaemmaghami et al. 2003), and the comparative expression data from (Gomar-Alba et al. 2015) (GEO access number: GSE59569), which determined the relative concentration of RTG proteins. Third, a random search method was applied to explore the parameter set. Finally, the steady states of the model were compared to

the Boolean model. A parameter set was regarded as valid when the steady states fulfilled the observations of 17 knockout conditions from (Sekito et al. 2000) and (Sekito et al. 2002).

A differential equation-based model can be used to simulate the dynamics of mitochondrial signaling and understand the communication characteristics associated with RTG protein regulation under stress. The behavior of the model is also informative of biological noise and can be further modified as per the Langevin equation for stochastic simulation. The deterministic model describes the tendency of a given state. Furthermore, steady states can be verified via GFP localization (Sekito et al. 2000, 2002).

The ultrasensitivity of Bmh/Mksp degradation causes a switch-like response of Rtg1/3p to mitochondrial damage

As described, nuclear accumulation of Rtg1p and Rtg3p activates the retrograde response. Their translocation results from mitochondrial damage, which activates Rtg2p and further induces the degradation of Bmh/Mksp. However, the mechanism by which information is propagated from the upstream Bmh/Mksp inhibitor to Rtg1/3p translocation remains unclear. To understand these dynamics, we applied a sigmoid signal of mitochondrial damage to simulate the transition of RTG proteins.

The step response revealed sophisticated details on RTG protein dynamics induced by the fast sigmoid transition of the damage signal (Figure 1b). The degradation of Bmh/Mksp indicated an ultrasensitive response to the input signal. However, the translocation of Rtg1p and Rtg3p was relatively smoother and delayed. Figure 1a indicates that a delayed response of Rtg1/3p translocation occurs with a sigmoid input. Further, Bmh/Mksp decreases rapidly after stimulation. The delayed stimulation of Rtg1p and Rtg3p may be caused by the slow Rtg3p autoactivation rate. Besides, the step responses overshoot pattern was identified in the particular forms of Rtg1p and Rtg3p, while summation canceled this effect (Figure S2).

Two forces control the nuclear translocation of Rtg3p, namely autoactivation of the nuclear localization signal (NLS) and degradation of the cytoplasmic Rtg1/3p heterodimer, releasing extra Rtg3p monomers that permeate the nuclear membrane. When the mitochondrial damage signal degrades Bmh/Mksp via Rtg2p, the autoactivation of Rtg3p turns on the NLS and increases the influx kinetic coefficient. Furthermore, the overshoot of activated Rtg3p concentration causes the decline observed in the early response (Figure S2). The decreased cytoplasmic Rtg3p concentration causes further degradation of the Rtg1/3p heterodimer, releasing more free Rtg3p. Autoactivation of the Rtg3p NLS contributes to the sharp increase in Rtg3p nuclear concentration shortly after the damage signal. Once autoactivation reaches a steady-state, free Rtg3p is conserved and translocated to the nucleus by simple diffusion. Hence, the transition of Rtg3p becomes smoother in the second stage, leading to a capacity-charging curve at the end (See Figure S3). In addition to Rtg3p, the

translocation of Rtg1p also results from degradation of the cytoplasmic Rtg1/3p heterodimer and simple diffusion. When Rtg1p is absent or negligible, simple diffusion causes Rtg3p to accumulate in the nucleus independently of the damage signal. The role of Rtg1p is to retain Rtg3p in the cytoplasm, however, the anchoring force is insufficient to retain activated Rtg3p (Sekito et al. 2000). The current simulation supports previous observations and provides details regarding the ultrasensitivity of Bmh/Mksp degradation, the two-staged transition of Rtg3p, and the capacity-charging curve of Rtg1p in response to mitochondrial damage signals.

Competitive Mksp binding between Bmhp and Rtg2p contributes to the ultrasensitivity of Bmh/Mksp degradation

The ultrasensitivity of Bmh/Mksp degradation is indicated by the phase plot with mitochondrial damage as input (Figure 2). The damage signal induces Rtg2p activation. Although the Hill function models this process with a dissociation constant k_{nd}, the phase plot of Rtg2p revealed a two-staged sigmoid transition with two dissociating constants significantly below k_{nd}, and with higher stiffness on the first one(Figure 3). The degradation of Bmh/Mksp occurs at the first transition, wherein the threshold for sensing mitochondrial damage is lower than that of the input Hill function. Therefore, the ultrasensitivity of Bmh/Mksp is independent of the Hill input model and is caused by the competitive binding between activated Rtg2p and Bmhp. To quantify the sigmoid-like transition sensitivity, the relative amplification method (Legewie et al. 2005), a quantitative approach for estimating the Hill coefficient with basal activation, was applied. As shown in Figure 3c, the response of inactive Rtg2p (Rtg2p^{ina}) was with lower Hill coefficients for both transitions compared to the input locally and globally (Figure 3c, left). Meanwhile, the degradation of the Bmh/Mksp heterodimer occurs at the first transition of Rtg2p^{ina}, with a higher Hill coefficient, which was lower than that of the input (Figure 3c, right). Via the relative amplification method, we estimated the Hill coefficient numerically. Despite knowing the quantity of the Hill coefficient, the transition of Bmh/Mksp occurred far below the dissociation constant k_{nd}, which is unlikely to be caused by the input Hill function, leading to questions regarding the source of its ultrasensitivity. To elucidate the underlying mechanism, we analyzed the Rtg2p-Mksp-Bmhp motif by solving the steady states algebraically. The exact analytical solution revealed that the transitions of inactivated Rtg2p stem from the molecular titration (see section S2 for details). Furthermore, the competitive binding between Rtg2p and Bmhp with Mksp form a binary switch that could process the analog input signal into digital information.

Frequency modulation of mitochondrial retrograde signaling

In addition to the binary response, we further investigated the input-output relationship in the frequency domain. Figure S6 depicts the frequency modulation of the Bmh/Mksp heterodimer, as

well as nuclear Rtg1p, and Rtg3p in response to a sinusoidal damage signal of multiple frequencies, all of which exhibited low-pass filter behavior. The recovery rate of Bmh/Mksp synthesis was slower than its degradation (Figure S6a), leading to a sign-sensitive delay that keeps the switch on after damage is detected (Alon 2019), while Bmh/Mksp can be slowly synthesized for a long period of approximately 3×10^3 seconds compared to the transition of less than 10 seconds (See Figure S8a). Although the concentration of Bmh/Mksp recovers slowly after stimulation, Rtg1p and Rtg3p are still able to convey input signal dynamics (Figure S6b and S6c). At a low frequency, both reach high and low saturation states in a sinusoidal input cycle and produce a square wave pattern. As the frequency becomes high, the amplitude of output diminishes with drifting, indicating that mitochondrial damage signal is low-pass filtered by retrograde signaling. Moreover, the delay of RTG translocation may contribute to the instability and compromise robustness. To investigate the feedback instability of mitochondrial retrograde signaling, we further derived a Bode plot of the retrograde response in the stationary stage (Figure S7). In the frequency response of Bmh/Mksp, the gain decreased in two sections separated by $10^{-0.5}$ Hz. The gain of the high-frequency section decreased more rapidly than that of the low frequency, and the phase delay also increased significantly in the high-frequency region. The cutoff frequency of nuclear Rtg1p and Rtg3p was approximately 10^{-2} Hz as low-pass filters. For nuclear Rtg3p, there was a second cutoff frequency at approximately $10^{-0.5}$ Hz with a more rigid negative slope. In addition to the gain modulation, both nuclear Rtg1p and Rtg3p exhibited four sections of phase delay with increasing slope rigidity as the input frequency increased. Further, both shared similar cutoff frequencies at approximately $10^{-2.5}$, 10^{-2}, and 10^{-1} in phase delay (See the phase plots in Figure S7b and 4). Finally, we applied the Nyquist stability theorem to identify the closed-loop stability of mitochondrial retrograde signaling (See Nyquist section of Figure S7). Despite phase delay, retrograde signaling remained stable in response to the damage signal (Iglesias & Ingalls 2009). The phase and gain margin derived from the Bode plots can further indicate the tolerance of delay when retrograde signaling triggers a cellular response.

The intensity of the mitochondrial damage signal decreases the robustness of Rtg1/3p translocation

To understand how noise influences robustness along with the damage signal, the ODE model was further extended to chemical Langevin equations. The stochastic model incorporated the random process into a deterministic model, and the potential landscape of nuclear Rtg1/Rtg3p was derived by screening the damage input with ensemble simulations (Figure 5). Along with the damage signal, the sigmoid curve of the potential landscape was consistent with the deterministic results of Rtg1/Rtg3p (Figure 5b/S4a). Interestingly, the conjugated steady states were identified with yellow bands and the sigmoid curve (Figure 5b). This structure became distanced as the input

signal increased, indicating that noise was amplified and caused a larger bandwidth, leading to a compromised signal-to-noise ratio (SNR). Notably, three conjugated steady states were further investigated by measuring the output distribution for a given input (Figure 5). The three conjugated steady states were identified by the peak of the probability, which represented the high likelihood of the Rtg1/Rtg3p concentration in a given input. The conjugated steady states were located within the bandwidth of the probability density function (PDF), and the length of bandwidth was increased by the signal, as shown in Figure 5. This result suggests that mitochondrial retrograde signaling is not only a bistable model but a toggle-switch with three locally conjugated stable steady states and one saddle point (Figure 5c). In addition, the uncertainty of the output was worsened by a high input signal, which might compromise information relayed between mitochondria and the nucleus when the former continues to send high-intensity messages.

Discussion

The retrograde signaling pathway has been established as an important mechanism for mitochondrial quality control as it serves as both a sensor and reporter of the mitochondrial health status (Butow & Avadhani 2004). Quantitative and systemic analysis of this major communication channel will help us elucidate the crosstalk between mitochondria and the nucleus, which maintains cellular function under physiological and pathological conditions. Herein, we constructed a novel mathematical model of mitochondrial retrograde signaling in yeast, applying microscopic data of RTG pathway knockout experiments with gene and protein expression data for model validation. The differential equation-based model provides a comprehensive approach for studying the dynamic response of mitochondrial retrograde signaling, which has been experimentally challenging due to the lack of means for precise mitochondrial quality manipulation in real time. Retrograde signaling dynamics were observed after introducing the input signal with step and sinusoidal waveforms. Moreover, we applied an analytical solution to identify the source of ultrasensitivity in the degradation of the Bmh/Mksp heterodimer.

The switch-like behavior of the yeast RTG pathway was previously described by (Da Cunha et al. 2015). We validated switch-like behavior in our retrograde signaling model (Figure 1) through mathematical formulation and numerical simulation. We observed that switch-like behavior resulted from the competitive binding between active Rtg2p and Bmh. Besides, the effect of molecular titration triggered a two-staged transition in inactive Rtg2p. Ultrasensitivity is typical in cellular communication, allowing cells to remove noise and amplify input signals (Buchler & Louis 2008, Haney et al. 2010, Thattai & van Oudenaarden 2002). Rtg2p senses mitochondrial quality through the modulation of Bmhp and Mksp, facilitating detection via competitive binding. The "all-or-none" response can further filter the fluctuation and adjust to the unpredictable environment.

The current study further elaborates on the properties of signal modulation via Rtg1/3p translocation following static and sinusoidal damage signals. As described by (Sekito et al. 2000), Rtg1p acts as both a positive and negative regulator, retaining the transcription factor Rtg3p in the cytoplasm. This considerably constrains the valid parameter set (See Methods). Further mechanistic details were identified by the proposed model: the two-staged transition of Rtg3p translocation in step response and the sign-sensitive delay of Rtg3p with a short ON delay in oscillation signal. Without NLS modification, Rtg1p is required to retain Rtg3p in the cytoplasm when a mitochondrial damage signal is absent, which is one of the criteria of our model (See Methods). Rtg1p exerts an anchoring effect on Rtg3p by forming a heterodimer, which may not permeate through the nuclear membrane. The translocation of Rtg1p is not affected by the sign of the input change and reveals a simple diffusion process with a capacity-charging pattern. The frequency response further revealed the low-pass filtering of the RTG pathway, which can reject high-frequency fluctuations and retain the overall information of the input signal for requesting nuclear supply.

In the current study, we confirmed RTG signaling feedback stability via Bode and Nyquist diagrams (Iglesias & Ingalls 2009); the communication between mitochondria and the nucleus is a two-way process (Butow 2002): Further, retrograde signaling is connected to glutamate synthesis, mTOR signaling, and other feedback circuits (Butow & Avadhani 2004, Liu & Butow 2006, Whelan & Zuckerbraun 2013). The phase and gain margin in the Bode plot determined the stable region when cascading with these functional units under mitochondrial oscillation.

Our model also elucidates how the RTG pathway processes the input signal as a low-pass filter, reporting status to the nuclear genome, which may, in turn, support the synchronization of mitochondrial membrane potential in yeast (Lloyd et al. 2002, 2003, Murray et al. 2001) and insulin secretion from pancreatic cells (Heart et al. 2007). Moreover, mitochondria undergo energization cycles driven by the ultradian clock, contributing to respiratory oscillations of mitochondria (Lloyd et al. 2002, 2003, Murray et al. 2001). These oscillations may be a source of reactive oxygen species generated by mitochondria (Lloyd et al. 2003), and further interfere the retrograde signaling with sinusoidal input.

The mitochondrion acts as a biochemical signaling hub in eukaryotic cells (Chen et al. 2016). Apart from energy production, this semi-autonomous organelle also participates in various metabolic reactions related to aging (Christian & Shadel 2014, Miceli et al. 2012, Nyström 2013), cellular communication (Heart et al. 2007, Mottis et al. 2019) and cell viability (Fatima et al. 2020, Moye-Rowley 2005). The RTG pathway is a major factor in cellular adaptation, serving a cytoprotective role via metabolic reprogramming (Trendeleva & Zvyagilskaya 2018, Ždralević et al. 2012). The robustness of retrograde signaling is essential for adjusting to unfavorable conditions (Fatima et al. 2020). For instance, RTG signaling contributes to drug resistance in pathogenic yeast, such as *C. albicans*, which is responsible for approximately 80% of major systemic fungal infections (Badiee and Hashemizadeh, 2014, (Trendeleva & Zvyagilskaya 2018). Various antifungal drugs target

mitochondria-related amino acid and ergosterol metabolism (Jastrzebowska & Gabriel 2015, Pasko et al. 1990), while the RTG pathway enables pathogenic yeast to overcome therapeutic agents by sensing the loss of mitochondrial functionality and subsequently reprogramming their metabolism (Singh et al. 2018, Trendeleva & Zvyagilskaya 2018, Yan et al. 2014). Hence, the yeast retrograde signaling system represents a target for the development of novel antifungal drugs (Trendeleva & Zvyagilskaya 2018). However, how yeast senses mitochondrial stress via the RTG pathway in a dynamic environment remains unclear.

In this study, we applied mathematical modeling to unravel the dynamics of RTG signaling from a control system point of view. We further identified the threshold of the RTG response, which can be used for determining the optimal dosages for the elimination of pathogenic yeast without triggering RTG signaling. The frequency response reveals how yeast manages to resist fluctuation via low-pass filtering of the RTG pathway, as well as the hysteresis effect, which maintains retrograde signaling as the damage signal fluctuates, indicating that persistent treatment with a concentration slightly below the RTG response threshold is an optimal strategy against pathogenic yeast. Therefore, comprehensively understanding the qualitative properties of retrograde signaling may shed light on novel antifungal strategies.

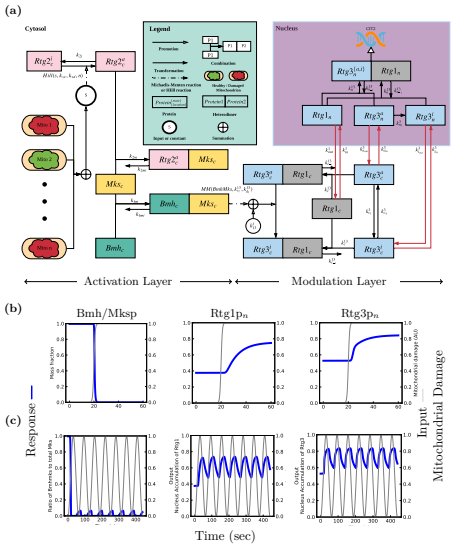

Figure 1. Mitochondrial retrograde signaling pathway model. (a) The mitochondria-to-nucleus communication circuit. Retrograde signaling is divided into the activation layer and modulation layer. Retrograde proteins (Bmhp, Mksp, and Rtg1/2/3p) are divided into an active (*-act*) and inactive state (*-ina*). Retrograde signaling begins with Rtg2p, which is a novel protein with an ATP-binding domain similar to the Hsp70/actin/sugar kinase superfamily. Rtg2p, a cytoplasmic protein, can be activated once the mitochondrion loses its membrane potential, or the ATP concentration decreases (Da Cunha et al. 2015, Ferreira et al. 2005, Liu & Butow 1999). The active form of Rtg2p suppresses the formation of the Mks/bmhp complex, an inhibitor of retrograde signaling, by binding with Mks1p, resulting in dephosphorylation of Rtg3p, which is a bHLH/Zip transcription factor associated with retrograde response genes (Ferreira et al. 2005, Liu & Butow 1999, Da Cunha et al. 2015). The mitochondrial retrograde response requires the presence of the Rtg1p-Rtg3p complex within the nucleus. When retrograde signaling is inactive, Rtg3p remains phosphorylated within the cytoplasm (Sekito et al. 2002). After the Bmh/Mksp complex is inhibited by active Rtg2p, Rtg3p tends to undergo dephosphorylation and translocates to the nucleus accompanied by Rtg1p. The Rtg1p-Rtg3p complex eventually triggers the retrograde response and upregulates *CIT2* (Liu et al. 2002, Sekito et al. 2000). Cellular compartments are divided based on the nucleus (*-nuc*) and cytosol (*-cyt*). In this model, the input s is defined as the summation of mitochondrial damage signals. The arrow represents the binding of two proteins, transformation of active states, or translocation be- tween nucleus and cytosol, with the kinetic coefficient labeled beside. The exact model of differential equations is described in section S1 of SOM. (b) Step responses of Bmh/Mksp, Rtg1p$_n$ and Rtg3p$_n$ showing switch-like responses of Bmh/Mksp, capacity-charging curve with a time delay for Rtg1p$_n$ and delayed two-staged rise with a sharp transition at the beginning, for Rtg3p$_n$. (c) The sinusoidal inputs of 1.6×10^{-2} Hz response reveals RTG signaling pathway as a low-pass filter. The mitochondrial damage signal (thin gray line), labeled as the input with quantity shown on the right y-axis. The concentration of RTG proteins (thick blue line), regarded as outputs with quantities labeled on the left y-axis. To normalize the response, the mass fraction is defined as the ratio of the concentration of a given protein set to its total concentration. Nucleus accumulation is described by the ratio of nucleus concentration to total protein concentration.

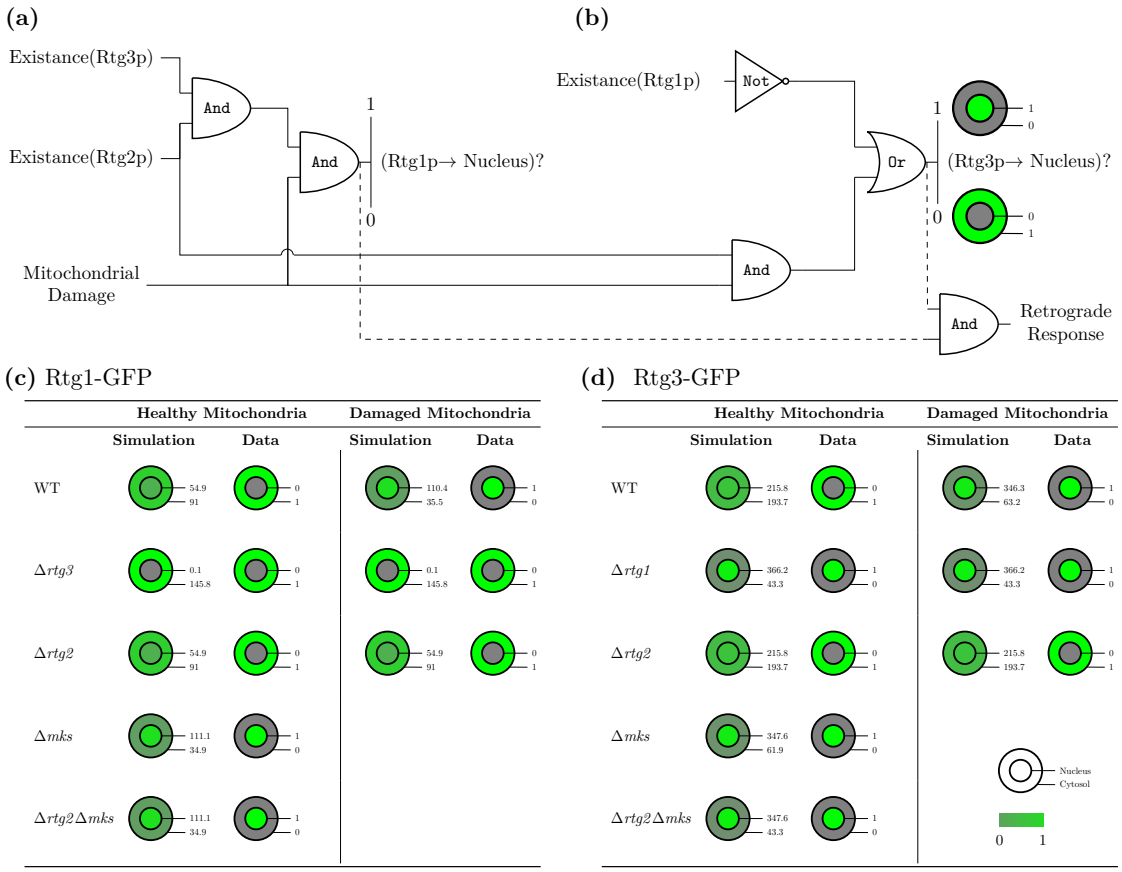

Figure 2. Boolean decision in RTG signaling pathway. (a) Logic gate analog for the RTG signaling pathway. Mitochondrial damage and the existence of Rtg1p Rtg2p, and Rtg3p determined translocation of Rtg1p and Rtg3p into nucleus though a series of logic gate decisions.(See Table S3 for details) (b) Boolean transformation of Rtg proteins nucleus translocation in healthy and damaged mitochondria. Simulation distribution of GFP-labeled RTG under multiple conditions compared to the Boolean model. The steady states of GFP proteins are listed by the cell icon labeled with nucleus and cytoplasmic concentration arbitrary units (inner and outer circles, respectively). Localized concentrations are the summation of protein species with GFP, including heterodimers. The relative quantity indicates the localized concentration-to-summation ratio, from 0 (gray) to 1 (green). To verify the result, simulated distributions are compared with the qualitative data aligned on the right side ((Δ*rtg1*/Δ*rtg2*/Δ*rtg3* from (Sekito et al. 2000) and Δ*mks* from (Ferreira et al. 2005) with binary labels, and 1 represents the higher concentration compared to the neighbor. Nuclear accumulation is regarded as a ratio of the nuclear-to-cytoplasmic concentration greater than 1.5.

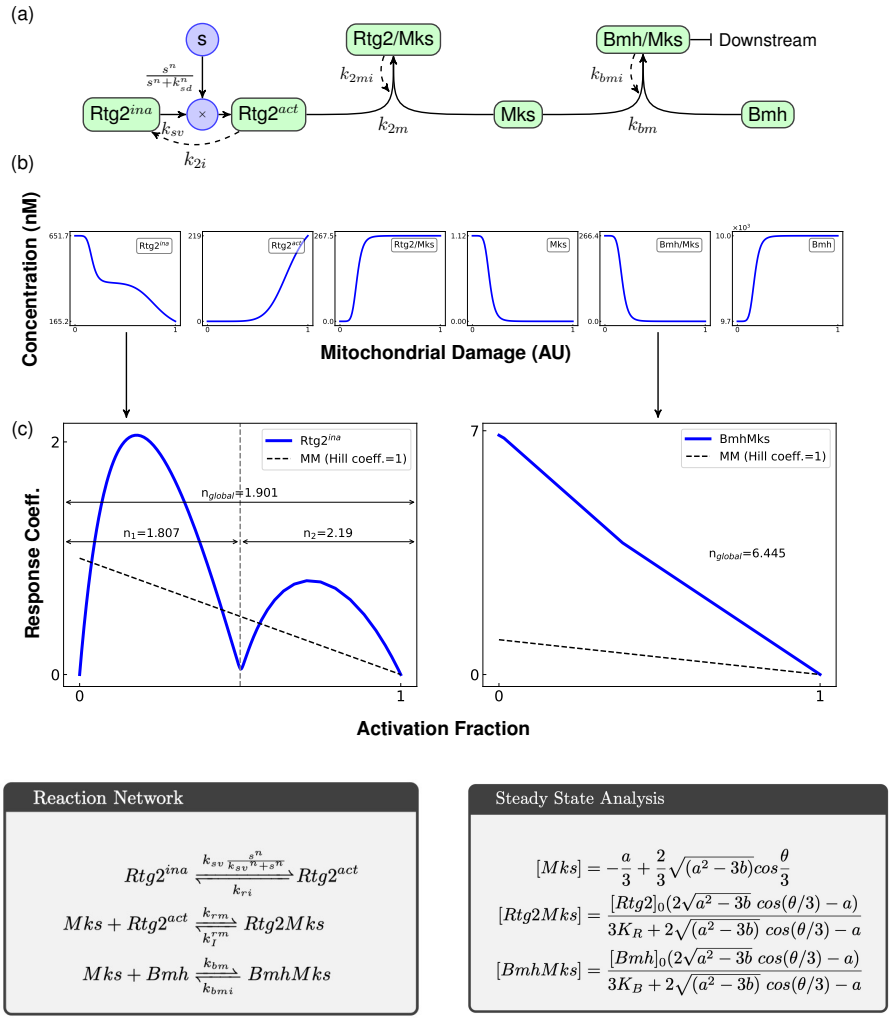

Figure 3. Ultrasensitivity of the Bmh/Mksp heterodimer results from molecular titration. (a) Scheme of the competitive Mksp binding between Rtg2p and Bmhp. The binding reactions and transformed processes are labeled with thick arrows with one or two ends, while reverse reactions are labeled with dashed arrows. (b) Phase plots of the input responses for $n = 7$, $k_{sd} = 0.96$,$k_{sv} = 11.67$, $k_{2i} = 4.94$, $k_{2mi} = 0.043$, $k_{2m} = 1604.15$, $k_{bmi} = 2.413$, $k_{bm} = 0.059$ with an arbitrary unit (AU). The input signal is defined within the interval between 0 and 1, and the corresponding steady states are plotted separately. (c) Relative amplification approach of Rtg2p^{ina} and Bmh/Mksp in response to mitochondrial damage input. The activated fraction is converted from the input signal s normalized by its range, as defined in (Legewie et al. 2005); the response coefficient is the normalized sensitivity of output with respect to the input signal (Ferrell & Ha 2014). The transformed responses of Rtg2p^{ina} and Bmh/Mksp (blue thick line) are compared via the Michaelis-Menten reaction with a Hill coefficient equal to one, which is a linear function (dashed line) (Legewie et al. 2005). n_{global} represents global Hill coefficient; n_1 and n_2 are local Hill coefficients in the first and second transition of Rtg2p^{ina} (See section S2 for details.).

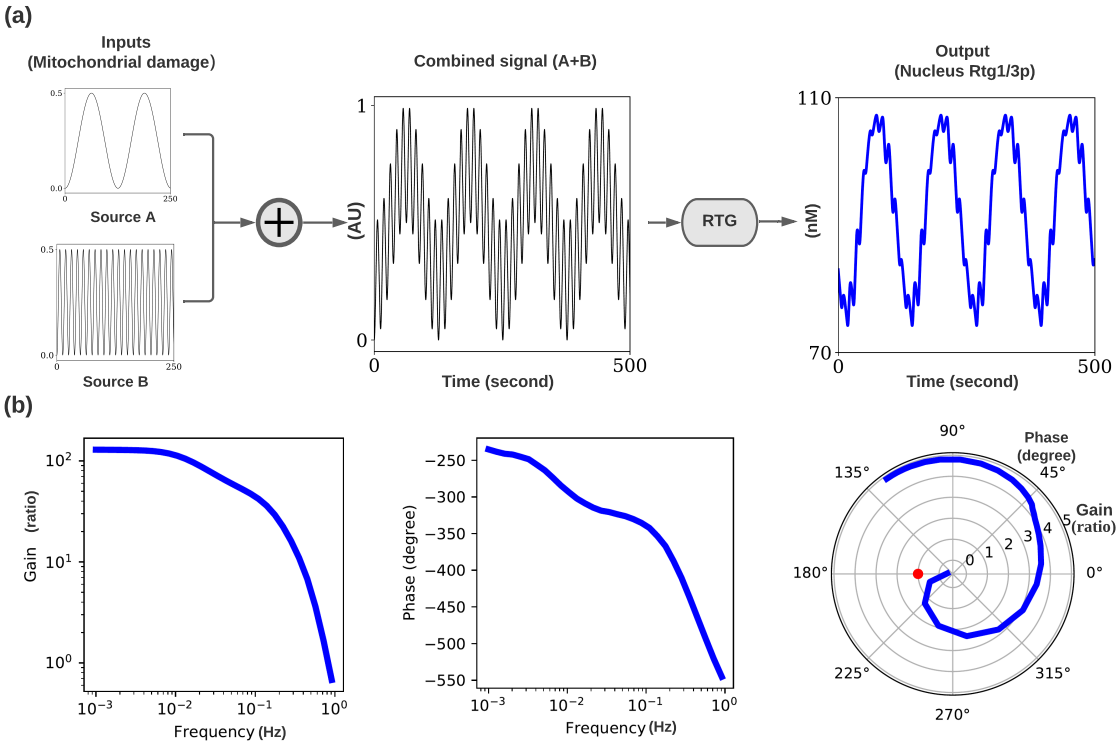

Figure 4. Frequency modulation of RTG pathway. (a) Multiplex processing of RTG signaling. The multiplexed signals from two individual mitochondria are low-pass filtered and delayed with respect to the frequency. The two inputs are set at 0.05 rad/s (source A) and 0.5 rad/s (source B) with the same phase. The overall effect on Rtg2p activation is summed with equal weights, and the combined signal is further modulated by the RTG pathway and detected by nucleus Rtg1/3p as the output. (see Figure S6 for details) (b) Frequency response to mitochondrial damage. (Left) Gain plot. Low-pass filtering is observed by screening the input frequency from 10^{-3} to 1 Hz with sinusoidal wave. The gain of nucleus Rtg3p is defined as the ratio of output to input amplitude measured by the peak-to-peak distance. (Middle) Phase plot. The delay of output is increased by the input frequency. With the time deviation between the peaks of output and input, the delayed Rtg3p signal is described by degrees in respect of the input frequency. (Right) The Nyquist plot, combined with the gain and phase plot, reveals the closed-loop stability of the proposed model. The radius represents the gain (dB), and the angle labels the degree of phase. The red dot represents the critical point $(-1 + 0i)$. The proposed model is stable if the Nyquist curve excludes the critical point (See Figure S7 for details).

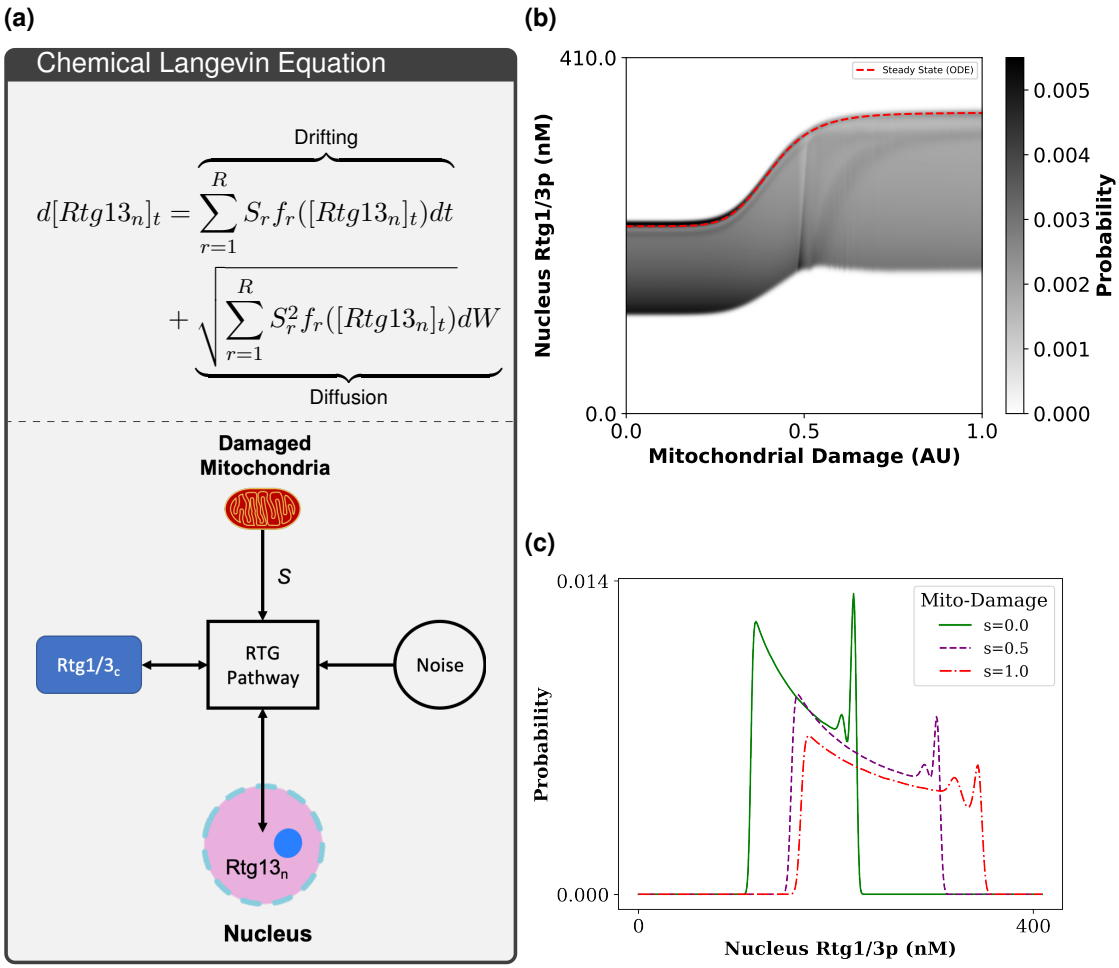

Figure 5. Robustness of Rtg1/3p translocation in response to mitochondrial damage signal. (a) The potential landscape of the nuclear Rtg1/Rtg3p response to mitochondrial damage signals. The sigmoid transition is identified in Figure S4a, however, the bandwidth (the yellowish area in the vertical section) increases in parallel to the damage signal. The damage signal is sampled in 100 grids and assigned to the chemical Langevin model in order to simulate the stochastic process. Every combination of parameters is applied with 100-time length (arbitrary unit) with automatic time step. The y-axis is limited within the range of 0 and the maximum concentration of Rtg3p. A heatmap shows the probability with a color bar on the right side. (See Methods for details.) (b) The probability density function (PDF) with respect to Rtg1/Rtg3p influenced by damage signal. The distribution is simulated by setting the input signal as 0 (blue, minimal input), 0.45 (orange, intermediate input), and 1 (green, maximum input). The peaks represent three stable steady states, and the valley between the right two high peaks is the saddle point. The PDF is measured by time series simulation and estimates the probability via kernel density estimation

Methods

Boolean Model of Mitochondrial Retrograde Signaling

To summarize the systematic behavior of mitochondrial retrograde signaling, a Boolean model was established to discretize the mechanism of protein translocation associated with mitochondrial damage. In this model, The population of N mitochondria is indexed into a vector $\vec{MT}$(Eq. 1).

$$\vec{MT} := [MT_1, ..., MT_N] \tag{1}$$

Though it is known that damaged mitochondria activate Rtg2p and promote the dephosphorylation of Rtg3p by decreasing the Bmh/Mksp heterodimer (Jazwinski & Kriete 2012, Sekito et al. 2000), how Rtg2p senses mitochondrial dysfunction remains unclear. Therefore, we assume mitochondria activates Rtg2p simultaneously under Michaelis-Menten kinetics (Ingalls 2013, pp. 356), and the activation rate of Rtg2p is influenced by the weighted linear summation of mitochondrial damage signals (S) with their volume(Eq. 2).

$$S = \sum_{i=1}^{N} Volume_{MT_i} \times Damaged_{MT_i} \tag{2}$$

In our Boolean model, the signal (S) is set to 0 for the healthy mitochondrial population and to 1 when mitochondria are damaged, as in ρ^0 yeast cells which have no mitochondrial DNA. These genetically damaged mitochondria have no respiratory functionality and constitutively activate retrograde signaling, which causes the translocation of Rtg1p and Rtg3p, when cells contain intact RTG components (Table S1). The translocation of Rtg1p and Rtg3p can turn on the retrograde response, including the upregulation of *CIT2* (Jazwinski & Kriete 2012).

(Sekito et al. 2000) determined the nuclear concentration of Rtg1p, Rtg2p and Rtg3p relative to cytoplasmic levels via GFP labeling, RTG knockouts, and the comparison between rho$^+$ and rho^0 cells. Therefore, the translocation event, existence of RTG components, and mitochondrial functionality can be summarized into a Boolean table, describing the system behavior of the RTG signaling pathway (Table S2). The Boolean relation between mitochondrial damage (input) and the translocation of Rtg1p or Rtg3p can be further simplified with a logically equivalent (Figure 2(a,b)).

$$\begin{aligned} [*-Rtg1_C] &:= [Rtg1_C] + [Rtg1 - Rtg3_C^P] + [Rtg1 - Rtg3_C^U] \\ [*-Rtg1_N] &:= [Rtg1_N] + [Rtg1 - Rtg3_N^P] + [Rtg1 - Rtg3_N^U] \\ [Rtg3_\#^*] &:= [*-Rtg3_C^*] + [*-Rtg3_N^*] \end{aligned} \tag{3}$$

Expression of RTG genes

The expression level of RTG genes under osmotic stress was measured via RNA-seq. The data was analyzed by the discrete distributional differential expression (D3E), a tool for the analysis of single-cell RNA-seq data (Delmans & Hemberg 2016). We also used the quantitative western blot results from (Ghaemmaghami et al. 2003) for determining the total concentration of RTG proteins.

From Boolean model to an ordinary differential equation-based model

In order to investigate information transmission properties, an ordinary differential equation-based model of mitochondrial retrograde signaling was developed to simulate the biological process of mitochondrial retrograde signaling. The following sections describe the differential equation-based framework of the yeast RTG pathway (Figure 1).

Reactions of mitochondrial retrograde response were derived based on the law of mass action and Michaelis-Menten kinetics.

The activation layer consists of Rtg2p, Mksp, as well as Bmhp, and conveys the mitochondrial damage signal via Rtg2p activation and suppression of the Bmhp-Mksp heterodimer which is an inhibitor of the RTG pathway. Later on, Rtg1p and Rtg3p form the modulation layer. Rtg3p contains an NLS and is poly-phosphorylated when the RTG pathway is inactive. In contrast, upon mitochondrial damage, Rtg3p is less phosphorylated and tends to translocate into the nucleus. The process of transcription factor translocation of modeled with simplified mass kinetics (Eq. 4) as previously described (Hao et al. 2013).

$$TF_c \underset{k_{out}}{\overset{k_{in}}{\rightleftharpoons}} TF_n \tag{4}$$

where TF_* represents transcription factor, and the subscripts $*$ describes the location with n representing nucleus and c representing the cytoplasm.

Parameter searching with the qualitative data of protein translocation

The parameters of Figure 1 determined the steady-state behavior with respect to mitochondrial damage. A valid parameter set should make the model fulfill all conditions observed in (Sekito et al. 2000) and (Liu et al. 2002) (Table S2). The parameter set was sampled in log-uniform with a fixed domain, and the relative amount of translocation kinetic coefficients is considered. To elaborate, the inward coefficient of nuclear Rtg3p with an active ($k^3_{a_{in}}$) was higher than the inactive one ($k^3_{i_{in}}$). Conversely, $k^3_{i_{out}}$ was higher than $k^3_{a_{out}}$ (Hao et al. 2013) (see Table S4).

The initial values of each component were sampled based on the expression level of RNA-seq expression levels (Figure S1). The relative amount of protein under both normal and stress

conditions was considered. The Boolean relations were tested by setting deleted proteins near zero, including modifications and complexes (see Section S1.4).

Once the parameters were sampled, the steady state of the model was derived by a dynamic solver, which provides an automatic switch between stiff and nonstiff algorithms when solving the differential equations. Furthermore, we chose the Order 2/3 L-Stable Rosenbrock-W method as the stiff solver, and the Tsitouras 5/4 Runge-Kutta method for the nonstiff section (Rackauckas & Nie 2017).

The unstable solutions were discarded if the iteration exceeded 10^6 with a deviation of derivatives beyond 10^{-8} in total. Further, the ratio of the nuclear concentration to cytoplasmic one was used to determine protein translocation. In our study, a nucleus-to-cytosol ratio larger than 1.5 was defined as a translocation event and vice versa. The translocation process under each deletion condition was compared with the Boolean model.

An Ordinary Differential Equation-based Model of Mitochondrial Retrograde Signaling in Yeast

As illustrated in Figure 1, The input layer was composed of an inactive form of Rtg2p (Rtg2p$_C^{ina}$), and the active form of Rtg2p (Rtg2p$_C^{act}$). Both of them were always cytoplasmic (C). As mentioned above, Rtg2p is the sensor of mitochondrial damage (Ferreira et al. 2005, Liao & Butow 1993, Rios-anjos et al. 2017), and its activation is caused by loss of mitochondrial membrane potential or an insufficient ATP cytoplasmic concentration (Rios-anjos et al. 2017). This process is modeled via the Michaelis-Menten equation (Ingalls 2013) (See Table. S4 for details).

Stochastic simulation of Rtg1/3p translocation in response to mitochondrial damage

The stochastic model is modified from the ordinary differential equations with the theory of Chemical Langevin Equation (CLE) (Gillespie 2000). The derivative of nucleus Rtg1/3p is composed of the drifting term from the deterministic model, and the diffusion term caused by the Brownian motion. The process is described with the stochastic differential equation in Equation 5.

$$d[Rtg13_n]_t = \underbrace{\sum_{r=1}^{R} S_r f_r([Rtg13_n]_t)dt}_{\text{Drifting}} + \underbrace{\sqrt{\sum_{r=1}^{R} S_r^2 f_r([Rtg13_n]_t)}dW}_{\text{Diffusion}} \tag{5}$$

where f_r is the propensity of rth reaction, S_r the net change of the reaction r, and dW represents the Wiener process (Schnoerr et al. 2014).

The CLE was solved by Euler-Maruyama method with adaptive time stepping, and simulated for 100 seconds of time span. Furhter, the time series simulation was used to derived the likelihood of the output state with kernel density estimation as illustrated in Figure 5.

References

Alon, U. (2019), An introduction to systems biology: design principles of biological circuits, CRC press, pp. 37–54.

Aon, M. A., Bhatt, N. & Cortassa, S. C. (2014), 'Mitochondrial and cellular mechanisms for managing lipid excess', *Frontiers in physiology* **5**, 282.

Buchler, N. E. & Louis, M. (2008), 'Molecular titration and ultrasensitivity in regulatory networks', *Journal of molecular biology* **384**(5), 1106–1119.

Butow, R. a. (2002), 'Cellular responses to mitochondrial dysfunction: it's not always downhill.', *Cell death and differentiation* **9**(10), 1043–5.

Butow, R. A. & Avadhani, N. G. (2004), 'Mitochondrial signaling: The retrograde response', *Molecular Cell* **14**(1), 1–15.

Cagin, U. & Enriquez, J. A. (2015), 'The complex crosstalk between mitochondria and the nucleus: What goes in between?', *International Journal of Biochemistry and Cell Biology* **63**(February), 10–15.

Chelstowska, A., Liu, Z., Jia, Y., Amberg, D. & Butow, R. A. (1999), 'Signalling between mitochondria and the nucleus regulates the expression of a new D-lactate dehydrogenase activity in yeast', *Yeast* **15**(13), 1377–1391.

Chen, W. W., Freinkman, E., Wang, T., Birsoy, K. & Sabatini, D. M. (2016), 'Absolute Quantification of Matrix Metabolites Reveals the Dynamics of Mitochondrial Metabolism', *Cell* pp. 1324–1337.

Christian, B. E. & Shadel, G. S. (2014), 'Aging: It's SIRTainly possible to restore mitochondrial dysfunction', *Current Biology* **24**(5), R206–R208.

Cover, T. M. & Thomas, J. A. (2005), *Elements of Information Theory*, Wiley.

Da Cunha, F. M., Torelli, N. Q. & Kowaltowski, A. J. (2015), 'Mitochondrial Retrograde Signaling: Triggers, Pathways, and Outcomes', *Oxidative Medicine and Cellular Longevity* **2015**.

Delmans, M. & Hemberg, M. (2016), 'Discrete distributional differential expression (D3E) - a tool for gene expression analysis of single-cell RNA-seq data', *BMC Bioinformatics* **17**(1), 110.

Epstein, C. B., Waddle, J. A., Hale IV, W., Davé, V., Thornton, J., Macatee, T. L., Garner, H. R., Butow, R. A., Iv, W. H., Davé, V., Thornton, J., Macatee, T. L., Garner, H. R. & Butow, R. A. (2001), 'Genome-wide responses to mitochondrial dysfunction', *Molecular Biology of the Cell* **12**(2), 297–308.

Fatima, Z., Kumar, B., Rehman, S. & Hameed, S. (2020), Retrograde signaling: A novel antifungal drug target, *in* 'New and Future Developments in Microbial Biotechnology and Bioengineering', Elsevier, pp. 219–226.

Ferreira, J. R., Spírek, M., Liu, Z. & Butow, R. A. (2005), 'Interaction between Rtg2p and Mks1p in the regulation of the RTG pathway of Saccharomyces cerevisiae', *Gene* **354**(1-2 SPEC. ISS.), 2–8.

Ferrell, J. E. & Ha, S. H. (2014), 'Ultrasensitivity part I: Michaelian responses and zero-order ultrasensitivity'.

Friedman, J. R. & Nunnari, J. (2014), 'Mitochondrial form and function', *Nature* **505**(7483), 335–343.

Gabaldón, T. & Huynen, M. A. (2004), 'Shaping the mitochondrial proteome', *Biochimica et Biophysica Acta - Bioenergetics* **1659**(2-3), 212–220.

Ghaemmaghami, S., Huh, W.-K., Bower, K., Howson, R. W., Belle, A., Dephoure, N., O'Shea, E. K. & Weissman, J. S. (2003), 'Global analysis of protein expression in yeast', *Nature* **425**(6959), 737–741.

Gillespie, D. T. (2000), 'Chemical Langevin equation', *Journal of Chemical Physics* **113**(1), 297–306.

Gomar-Alba, M., Morcillo-Parra, M. A. & Olmo, M. L. D. (2015), 'Response of yeast cells to high glucose involves molecular and physiological differences when compared to other osmostress conditions.', *FEMS Yeast Research* **15**(5), fov039.

Haney, S., Bardwell, L. & Nie, Q. (2010), 'Ultrasensitive responses and specificity in cell signaling', *BMC systems biology* **4**(1), 119.

Hans, S., Fatima, Z. & Hameed, S. (2019), 'Retrograde signaling disruption influences ABC superfamily transporter, ergosterol and chitin levels along with biofilm formation in Candida albicans', *Journal de Mycologie Medicale* **29**(3), 210–218.

Hao, N., Budnik, B. A., Gunawardena, J. & O'Shea, E. K. (2013), 'Tunable signal processing through modular control of transcription factor translocation', *Science* **339**(6118), 460–464.

Hashim, Z., Mukai, Y., Bamba, T. & Fukusaki, E. (2014), 'Metabolic profiling of retrograde pathway transcription factors rtg1 and rtg3 knockout yeast.', *Metabolites* **4**(3), 580–98.

Heart, E., Yaney, G. C., Corkey, R. F., Schultz, V., Luc, E., Liu, L., Deeney, J. T., Shirihai, O., Tornheim, K., Smith, P. J. et al. (2007), 'Ca2+, nad (p) h and membrane potential changes in pancreatic β-cells by methyl succinate: comparison with glucose', *Biochemical Journal* **403**(1), 197–205.

Iglesias, P. A. & Ingalls, B. P. (2009), Control theory and systems biology, MIT Press, chapter 10.

Ingalls, B. P. (2013), *Mathematical Modelling in Systems Biology : An Introduction*, Vol. 53, pp. 149–180.

Jastrzebowska, K. & Gabriel, I. (2015), 'Inhibitors of amino acids biosynthesis as antifungal agents', *Amino acids* **47**(2), 227–249.

Jazwinski, S. M. (2013), 'The retrograde response: When mitochondrial quality control is not enough', *Biochimica et Biophysica Acta - Molecular Cell Research* **1833**(2), 400–409.

Jazwinski, S. M. & Kriete, A. (2012), 'The yeast retrograde response as a model of intracellular signaling of mitochondrial dysfunction', *Frontiers in Physiology* **3 MAY**(May), 1–12.

King, N. (2007), Amino acids and the mitochondria, *in* 'Mitochondria', Springer, pp. 151–166.

Knorre, D., Sokolov, S., Zyrina, A. & Severin, F. (2016), 'How do yeast sense mitochondrial dysfunction?', *Microbial Cell* **3**(11), 401–408.

Legewie, S., Blüthgen, N. & Herzel, H. (2005), 'Quantitative analysis of ultrasensitive responses', *FEBS Journal* **272**(16), 4071–4079.

Liao, X. & Butow, R. A. (1993), 'RTG1 and RTG2: Two yeast genes required for a novel path of communication from mitochondria to the nucleus', *Cell* **72**(1), 61–71.

Liu, Z. & Butow, R. a. (1999), 'A transcriptional switch in the expression of yeast tricarboxylic acid cycle genes in response to a reduction or loss of respiratory function.', *Molecular and cellular biology* **19**(10), 6720–8.

Liu, Z. & Butow, R. a. (2006), 'Mitochondrial retrograde signaling.', *Annual review of genetics* **40**, 159–185.

Liu, Z., Sekito, T., Epstein, C. B. & Butow, R. A. (2002), 'RTG-dependent mitochondria to nucleus signaling is negatively regulated by the seven WD-repeat protein Lst8p', *EMBO Journal* **20**(24), 7209–7219.

Lloyd, D., Eshantha, L., Salgado, J., Turner, M. P. & Murray, D. B. (2002), 'Respiratory oscillations in yeast: clock-driven mitochondrial cycles of energization', *FEBS letters* **519**(1-3), 41–44.

Lloyd, D., Lemar, K. M., Salgado, L. E. J., Gould, T. M. & Murray, D. B. (2003), 'Respiratory oscillations in yeast: mitochondrial reactive oxygen species, apoptosis and time; a hypothesis', *FEMS yeast research* **3**(4), 333–339.

Malina, C., Larsson, C. & Nielsen, J. (2018), 'Yeast mitochondria: An overview of mitochondrial biology and the potential of mitochondrial systems biology', *FEMS Yeast Research* **18**(5), 1–17.

Miceli, M. V., Jiang, J. C., Tiwari, A., Rodriguez-Quiñones, J. F. & Jazwinski, S. M. (2012), 'Loss of mitochondrial membrane potential triggers the retrograde response extending yeast replicative lifespan', *Frontiers in Genetics* **2**(JAN), 1–11.

Mottis, A., Herzig, S. & Auwerx, J. (2019), 'Mitocellular communication: Shaping health and disease', **366**(6467), 827–832.

Moye-Rowley, W. S. (2005), Retrograde regulation of multidrug resistance in saccharomyces cerevisiae, *in* 'Gene', Vol. 354, Gene, pp. 15–21.

Murray, D. B., Roller, S., Kuriyama, H. & Lloyd, D. (2001), 'Clock control of ultradian respiratory oscillation found during yeast continuous culture', *Journal of Bacteriology* **183**(24), 7253–7259.

Nyström, T. (2013), 'Aging: Filtering out bad mitochondria', *Current Biology* **23**(23), 1037–1039.

Osellame, L. D., Blacker, T. S. & Duchen, M. R. (2012), 'Cellular and molecular mechanisms of mitochondrial function', *Best Practice and Research: Clinical Endocrinology and Metabolism* **26**(6), 711–723.

Pasko, M. T., Piscitelli, S. C. & Van Slooten, A. D. (1990), 'Fluconazole: a new triazole antifungal agent', *Dicp* **24**(9), 860–867.

Rackauckas, C. & Nie, Q. (2017), 'Differentialequations.jl a performant and feature-rich ecosystem for solving differential equations in julia', *Journal of open research software* **5**.

Rios-anjos, R. M., Camandona, V. D. L., Bleicher, L. & Ferreira-junior, J. R. (2017), 'Structural and functional mapping of Rtg2p determinants involved in retrograde signaling and aging of Saccharomyces cerevisiae', pp. 1–27.

Rothermel, B. A., Thornton, J. L. & Butow, R. A. (1997), 'Rtg3p, a basic helix-loop-helix/leucine zipper protein that functions in mitochondrial-induced changes in gene expression, contains independent activation domains', *Journal of Biological Chemistry* **272**(32), 19801–19807.

Schnoerr, D., Sanguinetti, G. & Grima, R. (2014), 'The complex chemical langevin equation', *The Journal of chemical physics* **141**(2), 07B606_1.

Sekito, T., Liu, Z., Thornton, J. & Butow, R. A. (2002), 'RTG-dependent mitochondria-to-nucleus signaling is regulated by MKS1 and is linked to formation of yeast prion [URE3].', *Molecular biology of the cell* **13**(3), 795–804.

Sekito, T., Thornton, J. & Butow, R. A. (2000), 'Mitochondria-to-nuclear signaling is regulated by the subcellular localization of the transcription factors rtg1p and rtg3p.', *Molecular biology of the cell* **11**(6), 2103–15.

Singh, S., Fatima, Z., Ahmad, K. & Hameed, S. (2018), 'Fungicidal action of geraniol against candida albicans is potentiated by abrogated cacdr1p drug efflux and fluconazole synergism', *PloS one* **13**(8), e0203079.

Thattai, M. & van Oudenaarden, A. (2002), 'Attenuation of noise in ultrasensitive signaling cascades', *Biophysical journal* **82**(6), 2943–2950.

Trendeleva, T. & Zvyagilskaya, R. (2018), 'Retrograde signaling as a mechanism of yeast adaptation to unfavorable factors', *Biochemistry (Moscow)* **83**(2), 98–106.

Whelan, S. P. & Zuckerbraun, B. S. (2013), 'Mitochondrial signaling: Forwards, backwards, and in between', *Oxidative Medicine and Cellular Longevity* **2013**, 1–10.

Yan, H., Zhao, Y. & Jiang, L. (2014), 'The putative transcription factor cartg3 is involved in tolerance to cations and antifungal drugs as well as serum-induced filamentation in candida albicans', *FEMS yeast research* **14**(4), 614–623.

Ždralević, M., Guaragnella, N., Antonacci, L., Marra, E. & Giannattasio, S. (2012), 'Yeast as a Tool to Study Signaling Pathways in Mitochondrial Stress Response and Cytoprotection', *The Scientific World Journal* **2012**, 1–10.